CRATER SIZE–FREQUENCY DISTRIBUTIONS OF INTERIOR AND EXTERIOR UNITS AT GIORDANO BRUNO. A. R. Kubas[1], M. Zanetti[2], C. W. Hamilton[1], J. R. C. Voigt[1], J.-P. Williams[3], A. Pathare[3], E. S. Costello[4]. [1]Lunar and Planetary Laboratory, University of Arizona, 1629 E. University Blvd., Tucson AZ 85721, USA (alexiakubas@email.arizona.edu), [2]NASA Marshall Space Flight Center. [3]University of California, Los Angeles. [4]University of Hawai'i at Mānoa.

Introduction: Giordano Bruno is a young, Copernican-age crater on the lunar far side. With an estimated age of 1–10 Ma [1, 2], the surface is not old enough to have reached saturation. It is expected that a random distribution of craters will be expressed on its continuous ejecta blanket due to cratering by primary impactors. However, high-resolution images taken by the Lunar Reconnaissance Orbiter Camera (LROC) and previous crater-counting investigations revealed heterogeneities in the morphologies and spatial distribution of impact craters observed within the ejecta blanket and interior of Giordano Bruno [3, 4]. Here, we present a detailed examination of the point densities and crater size–frequency distributions (CSFDs) in different regions of the parent crater, its ejecta, and geomorphic mapped facies (Fig. 1). We explore factors that could have contributed to the observed crater densities, such as effects of post-formation impact melt mobility, self-secondary cratering (SSC), and target properties on small (D < 100 m) craters on the surface of Giordano Bruno.

Methods: *Crater Counts:* A total of 46,305 craters with diameters (D) of 10 to 290 m were digitized at a scale of 1:2,000 in ArcMap using the CraterTools plug-in [5]. The total count area was ~2500 km^2 and several subunits were included within. The basemap used was an LROC Narrow-Angle Camera (NAC) 1.8 m/pixel controlled mosaic image. Craters were counted down to 8 m in diameter to ensure the confidence that all craters with D > 10 m were incorporated, but craters with D < 10 m diameter were filtered out prior to analysis. A previous database of craters on the eastern and western flanks complemented this data set [6]. We counted all craters in the vicinity of Giordano Bruno crater (Fig. 1b), including areas not normally included in counts, such as the crater wall and floor. Counts included suspected secondary crater chains and clusters to determine density patterns across the entire crater and ejecta, but we have sorted these areas and craters for analyses sensitive to these data and are careful to declare when they are used.

Facies Map: The facies map (Fig. 2b) consists of 10 facies spanning the interior and exterior of Giordano Bruno. Explanations of each facies can be found in [7]. The "exterior" consists of all facies outside the crater rim boundary and "crater floor" consists of all facies inside the inner crater wall boundary.

Crater Densities: We used the point density tool in ArcMap to create the spatial density map [8] (Fig. 1a) using a search radius 564.2 m (i.e., 1 km^2 search area).

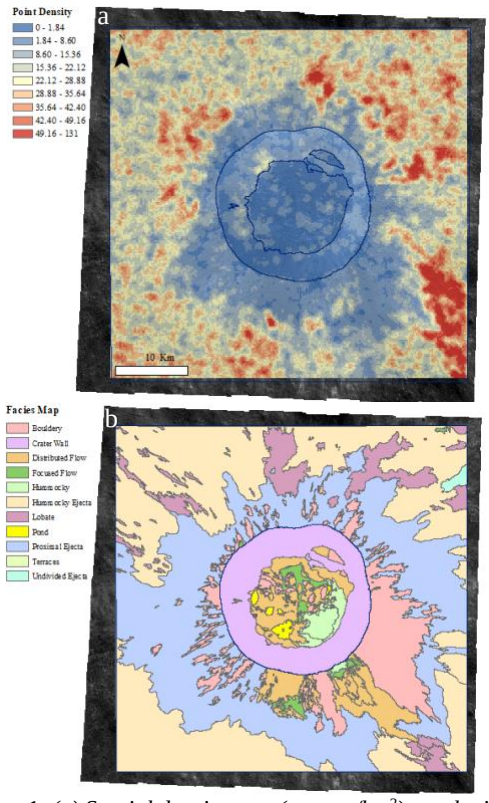

Figure 1: *(a) Spatial density map (craters/km^2) overlaying the LROC NAC mosaic basemap shown with total map, crater rim, and crater floor boundaries. (b) Facies map overlaying the basemap.*

To combat edge effects, the boundaries of the density map were buffered by the search radius and removed. Point density values were divided into 9 bins with ½ standard deviation widths (Fig. 1a). The lowest concentration of craters occur within the crater floor region and the densest concentrations occurs in the southeast sector of crater, within the proximal ejecta facies

CSFD Measurements: We used the Neukum 2001 production function in Craterstats2 to calculate the absolute model ages (AMAs) of all facies in Table 1 [9, 10]. Here we are using AMA (from N(1)) as a means of reporting CSFD measurement as it is helpful in cases of parent crater "age dating" where all facies should, in principle, show similar model ages, but do not and, additionally, for comparability with previous AMA estimates at Giordano Bruno [1,2].

Results: The exterior, crater wall, and crater floors of Giordano Bruno all have conflicting AMAs (Fig. 2). Compared to the exterior of the crater, the crater wall and floor have significantly fewer craters (in terms of both crater population and density). The crater floor unit's CSFD (Fig. 2, green square symbols) is much steeper than its corresponding best-fit isochron (Fig. 2, green line), and the unit has no craters with D > 20 m. The fit is poor because the observations do not match expected crater production. The crater floor of Giordano Bruno includes solidified impact melt ponds and boulder fields, making it a difficult terrain in which to count craters. Regardless, the paucity of craters on the crater floor indicates a significantly smaller population of craters likely formed there, and it is difficult to reconcile interior CSFD estimates with exterior estimates. Broadly, we find that crater interior units and exterior impact melt-related units (e.g., distributed flow, focused flow) display similarly low crater densities and AMAs relative to exterior ejecta units (e.g., proximal ejecta, lobate, etc.).

Discussion: For a population of primary impacts, AMAs should be similar for all ejecta, including impact melt deposits. There are several possible reasons for this, including target properties, real age differences, or self-secondary cratering [2]. Target property differences [e.g. 11] between facies may result in changes in crater diameter as measured in the CSFDs (and resulting AMA), but cannot fully explain the overall population difference and observed crater densities.

Thus, we suggest that impact melts in the crater interior and near the crater rim remained mobile after other parts of the impact ejecta came to rest, leading to SSC preservation being greater in the exterior of the crater than in the interior. Lev et al. [7] suggest the flow of impact melt generated during the formation of Giordano Bruno may have had an emplacement duration of ~76 hours. In comparison, the maximum flight time for an SSC is only ~48 minutes (using a simple ballistic on the Moon with a maximum velocity just below lunar escape velocity and an ejection angle of 85°). Thus, the impact melt deposits seen directly southeast of the crater rim and on the crater floor were not fully emplaced until after SSCs landed, which led to a lower apparent AMA. Interestingly, the crater wall also appears to have an older "age" than the crater floor. Our geomorphological investigations of the crater show that down-dropped terraces appear to have generated waves within the impact melt inside the crater, which would have led to the erasure of SSCs on the crater floor, relative to the crater walls. Thus, the chronology of impact crater facies appears to have involved an initial stage of broad ejecta blanket formation, followed by terrace collapse, and continued movement of initial impact melt emplacement, terracing, and continued melt mobility inside and outside the crater. During this time SSCs would have been raining down on all surfaces but were only preserved where surfaces were fully at rest. This chronology is supported by the CSFDs (Fig. 2) and shows how combining detailed geomorphic facies mapping and crater counting/CSFD analyses can be used to discern timing of events during the cratering process.

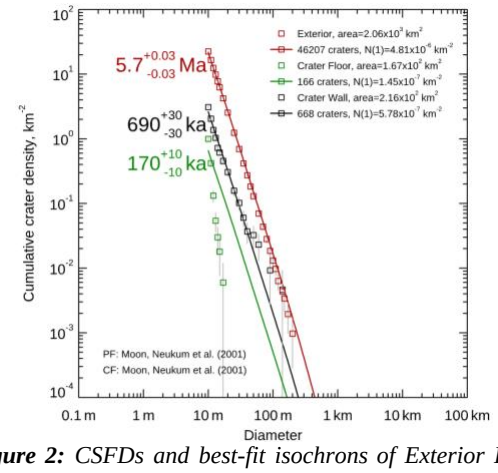

Figure 2: *CSFDs and best-fit isochrons of Exterior Facies, Crater Wall, and Crater Floor. The green line is the best -fit isochron and not a regression through the data. The fit is poor.*

Facies	AMA	N(1) (km⁻²)	# Craters	Area (km²)	Mean # Density (km⁻²)
Pond	55 ka	4.67E-08	3	11.59	0.26
Hummocky	400 ka	3.41E-07	75	34.75	2.16
Crater Wall	690 ka	5.78E-07	669	215.97	3.10
Focused Flow	750 ka	6.35E-07	84	27.56	3.05
Distributed Flow	1.4 Ma	1.20E-06	836	163.11	5.13
Bouldery	2.3 Ma	1.94E-06	1751	243.51	7.19
Proximal Ejecta	4.2 Ma	3.55E-06	18186	785.79	23.14
Lobate	5.6 Ma	4.71E-06	3302	145.12	22.75
Hummocky Ejecta	6.7 Ma	5.67E-06	22185	804.94	27.56
Undivided Ejecta	7.6 Ma	6.46E-06	228	6.78	33.63

Table 1: *Facies and their AMAs calculated in Craterstats2, with N(1), number of craters, area, and mean number density.*

Acknowledgements: This work was supported by a NASA cooperative agreement awarded to the Arizona/NASA Space Grant Consortium and NASA LDAP Program Grant # 80NSSC19K0871. Any opinions, findings, conclusions, or recommendations expressed in this material are those of the author and do not necessarily reflect the views of NASA.

References: [1] Morota T. et al. (2009) *Meteoritics & Planet. Sci., 44*, 1115–1120. [2] Plescia J., Robinson M. (2019) *Icarus, 321*, 974–993. [3] Plescia J. et al. (2010) *LPSC XLI*. [4] Williams J.P. et al. (2014) *LPSC XLV*. [5] Kneissl T. et al. (2011) *Plant. Space Sci., 59*, 1243–1254. [6] Williams J.P. et al. (2020) *11th Crater Consortium*. [7] Lev E. et al. (2021) *Icarus, 369*. [8] Silverman, B., (1986) *Monographs on Statistics and Applied Probability*. [9] Neukem G. et al. *Chronol. Evol. Mars., 96*, 55–86. [10] Michael G. (2010) *Earth Planet. Sci. Lett., 294*, 223–229. [11] van der Bogert, C. et al. (2017) *Icarus, 298*, 49–63.